

Pn Q UNDER TIBET AND TIENSHAN WITH PRACTICAL AND SCIENTIFIC IMPLICATIONS

Jiakang Xie

Lamont-Doherty Earth Observatory, Columbia University

Sponsored by Defense Threat Reduction Agency

Contract No. DTRA01-00-C-0048

ABSTRACT

Pn waves from three near-co-located seismic events in the eastern Tarim Basin are well recorded by seismic arrays in Kyrgyzstan and the central and southern portions of the Tibetan Plateau. These events include two underground nuclear explosions from 1994 and one nearby earthquake from 1999, all with similar magnitudes (~5.9). Pn waves recorded at the Kyrgyzstan and Tibetan (INDEPTH) arrays sample the uppermost mantle under the Tianshan and Tibetan plateaus, respectively, and have similar distance ranges of ~1,000 km. Pn wave arrival times are used to estimate high-apparent velocities of 8.3– 8.4 km/s under the Kyrgyzstan and southern Tibetan arrays, and low-apparent velocities of about 7.6 km/s under the north central Tibet array. Pn amplitudes are highly variable across the Kyrgyzstan array (by a factor of ~19). When stacked across the arrays, the average Pn wave amplitude over the Tianshan and Tibetan paths have very similar levels at low frequencies (~0.3 Hz). With increasing frequency, the average amplitudes over the Tibetan paths become lower and lower as compared to those over the Tianshan paths. At 4 Hz the average amplitudes over the Tibetan paths drop to a factor of 40, lower than those over Tianshan paths. The Pn wave source spectra can be successfully modeled by the modified Mueller-Murphy (MMM) and Brune source models for the explosions and the earthquake, respectively. A spectral overshoot near the corner frequencies (between 1-2 Hz) in the MMM source model is required to fit the explosion spectra. Pn attenuation can be modeled by a Pn Q that follows a power-law frequency dependence. We estimated the Pn Q_0 (Pn Q at 1 Hz) to be 30% higher over the Tianshan paths than over the Tibetan paths. We found the most striking difference is the power-law exponent η values; η is ~0.5 over the Tianshan paths and is ~0 over the Tibetan paths.

A practical implication of our result is that when we attempt to identify explosions with seismic data over paths with an Lg blockage, we may take advantage of the spectral overshoot that is present in the explosion Pn source spectra but absent in the earthquake source spectra. Array data is highly desirable owing to the inherent instability of Pn wave amplitudes. A scientific implication is that a melt-bearing uppermost mantle, such as that under Tibet, may have a frequency-independent P wave Q. This frequency independence is in direct contrast with the normal, “dry” uppermost mantle in which P wave Q is moderately dependent on frequency.

OBJECTIVE

The primary objective of this research is to quantify propagation and attenuation of high-frequency regional waves in and around the Tibetan plateau. We wish to measure the laterally-variable Pn and Lg Q and the travel times of Pn waves from events in the southern and central Tarim Basin of Tibet. Additionally, we wish to invert fundamental-mode surface waves to obtain depth variations of crustal Q in localized regions inside the plateau, such as the regions behind the vast Himalayas where Lg blockage appears to take place.

This research provides important data for the worldwide monitoring of nuclear explosions. The Q and travel times can be used for estimating source spectral characteristics and locations of any future seismic events to infer their nature and size. A comparison of the source spectra of explosions and earthquakes, estimated using the Pn over Tibetan paths, allows us to test the possibility of identifying the source type using the Pn alone when the Lg and Sn waves are blocked. Details of the lateral variations of Q will also enable us to search for a physical mechanism, such as a molten crust or upper mantle, that is responsible for the severe attenuations of regional waves in complex, low-Q regions of the world.

RESEARCH ACCOMPLISHED

Data Processing

We collected Pn waveforms from three nearby co-located seismic events in the eastern Tarim Basin. These events include two underground explosions on June 10 and October 7, 1994 with an mb of 5.7 and 5.9, respectively; and an earthquake on January 30, 1999 with an mb of 5.9 (Figure 1). The two explosions were recorded by multiple portable stations deployed in southern Tibet during the 1994 INDEPTH II PASSCAL experiment. The earthquake was recorded by stations deployed in the central and southern regions of Tibet during the 1999 INDEPTH III experiment. All three events were also recorded at the Kyrgyzstan network (KNET), which is located to the west of the events and consists of eleven broadband stations. As shown in Figure 1, Pn to the INDEPTH stations travels southward, mainly sampling the uppermost mantle under Tibet. By contrast, Pn to the KNET stations travels westward, sampling the mantle under Tienshan. The distances in ranges to the INDEPTH and the KNET arrays are similar (roughly $1,100 \pm 200$ km). In this study, only vertical-component seismograms are used. Figure 2 shows examples of the record sections that contain Pn. On each record Pn arrival times are read. The Fourier amplitude spectra of Pn and early Pn coda are obtained by using multiple windows of 4.5 s with a 50% overlap (Xie and Patton, 1999). These spectra are then averaged to yield a stable spectral estimate of Pn and early Pn coda. From here on we will refer to the averaged spectra of Pn and early Pn coda as “Pn spectra”.

Apparent Pn Velocities Under Tibet and Tienshan

The Pn arrival times at the KNET and INDEPTH arrays are used to fit the apparent Pn velocities v_{app} , under these arrays (Figure 3). The values of v_{app} under the KNET are high (8.3 km/s or higher). Values of v_{app} under the INDEPTH II and the southern half of the INDEPTH III arrays, south of the Bangong-Niujiang Suture (BNS), in Figure 1) are also high (about 8.3–8.4 km/s). On the other hand, the value of v_{app} under the northern half of the INDEPTH III array is low (about 7.7 km/s). This value is consistent with the previous discovery that the upper 100–150 km of the mantle under northern Tibet has slow P velocities (Zhao and Xie, 1993; McNamara et al., 1997).

Pn Amplitude Variability Across the Arrays

In the top panel of Figure 2, the time domain Pn amplitude varies by a factor of 19 across the KNET from the October 7 explosion. This instability of Pn amplitudes had been noticed before. Xie (1996) has explored extensively the origin of this instability and concluded that a Moho topography near the KNET is the most likely reason for this instability. Figure 4 shows a calculated ray pattern in the model that contains a Moho thinning, which might occur on the eastern side of the KNET as a deep signature of Lake Issyk-Kul. The ray focusing/defocusing in Figure 4 gives rise to an amplitude variability that is qualitatively similar to that observed in the top of Figure 2. The Moho thinning model in Figure 4 is 2-D and we anticipate even stronger focusing/defocusing if the Moho thinning has a more realistic 3-D shape.

Differences in Pn Attenuation Under Tibet and Tienshan

Figure 5 shows the Pn spectra from the October 7 explosion and the January 30 earthquake, both with an mb of 5.9. Similar to the time domain amplitude variability discussed earlier, the Pn spectra vary drastically by a factor of up to 10 for the INDEPTH and 20 for the KNET arrays, respectively, across each array. However, the array-average spectra (thick curves) start at similar levels at the lowest frequencies of about 0.3 Hz for different arrays recording the same event. Since the recording distances of the different arrays are similar (Figures 1 through 3), these similar low-frequency amplitudes of the array average mean that the uppermost mantle under Tibet and Tienshan have similar Pn attenuation rates. With increasing frequency the array-averages become more and more different than those from the INDEPTH arrays and lower than those from KNET. This difference means that the Tibetan mantle becomes increasingly more attenuated (compared to the Tienshan mantle) as the frequency increases. At 4 Hz in Figure 5, the INDEPTH array-average of Pn spectra is about 40 times lower than the KNET average. Another interesting phenomenon is that the explosion Pn spectra contains overshoot between 1–2 Hz, which is absent in the earthquake Pn spectra.

Following Xie and Patton (1999) we can quantify the above difference in Pn attenuation by assuming (1) a stochastic model of Pn spectra, (2) the modified Mueller-Murphy and Brune model for explosion and earthquake source spectra, respectively; and (3) a power-law frequency dependence of Pn Q:

$$Q_{Pn}(f) = Q_0 f^\eta$$

Using a Bayesian inverse method Xie and Patton (1999) estimated the moments and corner frequencies of Pn source spectra from the 1994 explosions; they also estimated Pn Q to the KNET stations from the explosion site (Lop Nor). In this study, we use these estimates as *a priori* knowledge to estimate the Pn Q to the INDEPTH arrays. The following Pn Q models are obtained:

$$Q_{Pn}(f) = (284 \pm 60) f^{(-0.1 \pm 0.2)}$$

from Lop Nor to INDEPTH II

$$Q_{Pn}(f) = (266 \pm 65) f^{(0.1 \pm 0.2)}$$

from Lop Nor to INDEPTH III, and

$$Q_{Pn}(f) = 364 f^{0.5}$$

from Lop Nor to KNET.

The 1-Hz Pn Q (Q_0) differs by about 30% under Tienshan and Tibet from the above equations. But Q_0 is not a good measure of how Pn Q differs under Tibet and Tienshan. This conclusion is so because in Figure 5 we see that Pn attenuation, or Q, should be roughly the same at the lowest frequencies of about 0.3 Hz. With increasing frequency, Pn Q under Tienshan and Tibet becomes more and more different. At 1 Hz the difference is minor compared to the difference at the higher frequencies. Fundamentally it is the frequency dependence, η , that characterizes the difference of Pn Q under Tibet and Tienshan; η is virtually 0 under the former and is moderate (about 0.5) under the latter. Previously, much of the Tibetan mantle traversed by Pn waves recorded at the INDEPTH arrays has been inferred to be partially molten based on studies of Pn velocity and Sn attenuation. By contrast, the Tienshan mantle is not a melt-bearing.

Practical and Scientific Implications

A practical implication of results of this study is that where regional S waves (e.g., Lg and Sn) are blocked, Pn spectra may be useful in event identification since explosion sources do, but earthquake sources do not, exhibit the spectral overshoot. Array data seem to be necessary in such a possible event identification to suppress the P-wave amplitude variability. Also, knowledge of Pn Q will be helpful because removing the path affect may enhance the source spectral signatures.

A scientific implication is that a melt-bearing mantle such as that under north and central Tibet may have an inherent physical property—that is, its bulk Q is nearly invariant between frequencies of a fraction of 1 Hz and a few Hz. This invariance contrasts with a dry mantle such as that under Tienshan in which bulk Q is moderately dependent on frequency. Recently Faul et al (2003) have conducted laboratory measurements of shear Q in olivine at seismic frequencies and upper mantle temperatures and pressures. They found that that a small fraction (<3%) of melt could produce a broad peak over which shear Q is independent of frequency. They infer that melt-bearing grain-boundary

gliding and diffusion may be the primary mechanisms for the shear wave energy loss. These microscopic mechanisms may be at work for bulk Q, as well.

CONCLUSIONS AND RECOMMENDATIONS

Pn waves from two explosions and a nearby earthquake in the eastern Tarim Basin have been recorded by arrays in Kyrgyzstan and central and southern Tibet. The respective Pn paths sample the uppermost mantle under the Tianshan and the Tibetan plateaus, respectively, at similar distances (around 1,000 km). Pn arrival times yield estimates of high-apparent velocities of 8.3–8.4 km/s under the Kyrgyzstan and southern Tibetan arrays, and low-apparent velocities of about 7.6 km/s under north central Tibet. Pn amplitudes are highly variable across each array (by factors of 10–20). When stacked over the arrays, the average Pn amplitudes over the Tianshan and Tibetan paths have very similar levels at low frequencies (~0.3 Hz). With increasingly higher frequencies, the average amplitudes over the Tibetan paths become increasingly lower as compared to those over the Tianshan paths. At 4 Hz the average amplitudes over the Tibetan paths drop to 40 times lower than those over Tianshan paths. The modified Mueller-Murphy and Brune source models can be used to successfully model the Pn source spectra for the explosions and earthquake. A spectral overshoot near the corner frequencies (between 1–2 Hz) is required to fit the explosion spectra. Pn Q is assumed to follow a power-law frequency dependence. We estimated Pn Q_0 (Pn Q at 1 Hz) to be 30% higher over the Tianshan paths than over the Tibetan paths. The most striking difference is found in η values; η is ~0.5 over the Tianshan paths and ~0 over the Tibetan paths.

Our results have both a practical implication in source identification using P waves and a scientific implication on an inherent frequency-independent bulk Q of the melt-bearing uppermost mantle. These implications lead to two recommended future works: (1) an exploration of whether it is feasible to use Pn or mantle P waves, recorded by arrays, to detect explosions which seem to exhibit spectral overshoots—such a use of P wave spectra for event identification may be necessary over paths of Lg and Sn blockage; and (2) measurements of bulk Q in the uppermost mantle in other regions not only to enhance our monitoring capability, but also to explore if an frequency-independent Q is a general, intrinsic property of the melt-bearing upper mantle.

REFERENCES

- Faul, U.H., J.D. Fitz Gerald and I. Jackson (2003), Shear-wave attenuation and dispersion in melt-bearing olivine polycrystals II. Microstructural interpretation and seismological implications, *J. Geophys. Res.*, submitted.
- McNamara, D., W.R. Walter, T.J. Owens, and C.J. Ammon (1997), Upper mantle velocity structure beneath the Tibetan Plateau from Pn travel time tomography, *J. Geophys. Res.*, **102**, 493-505.
- Roecker, S.W., T.M. Sabitova, L.P. Vinnik, Y.A. Burmakov, M.I. Golyanov, R. Mamatkanova, and L. Munirova (1993), Three-dimensional elastic wave structure of the western and central Tien Shan, *J. Geophys. Res.*, **98**, 15779-15795.
- Xie, J. (1996), Synthetic and observational study of Pn excitation and propagation in central Asia, *Phillips Laboratory Scientific Report No. 1*, PL-TR-96-2270, 24 pp.
- Xie, J. and H. Patton (1999), Regional Phase Excitation and Propagation in the Lop Nor Region of Central Asia and Implications for the Physical Basis of P/Lg Discriminants, *J. Geophys. Res.*, **104**, 941-954.
- Zhao, L.S. and J. Xie (1993), Lateral variations in compressional velocities beneath the Tibetan Plateau from Pn travel time tomography, *Geophys. J. Int.*, **115**, 1970-1084.

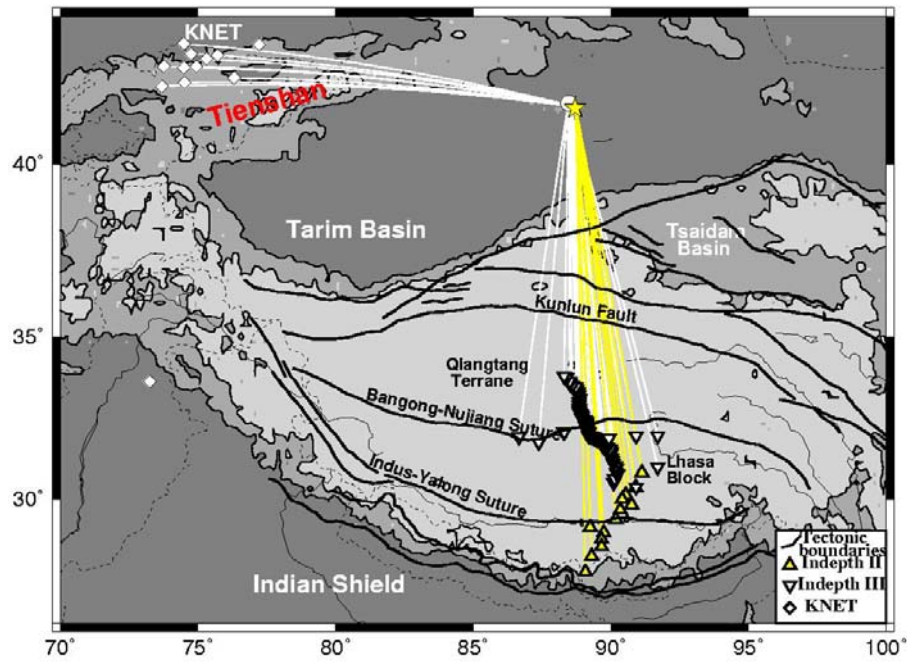


Figure 1. Map showing the tectonic and geographic features of the study area of the 1994 explosions (stars), the 1999 earthquake (circle), and KNET and INDEPTH stations (see legend), and the PN paths used.

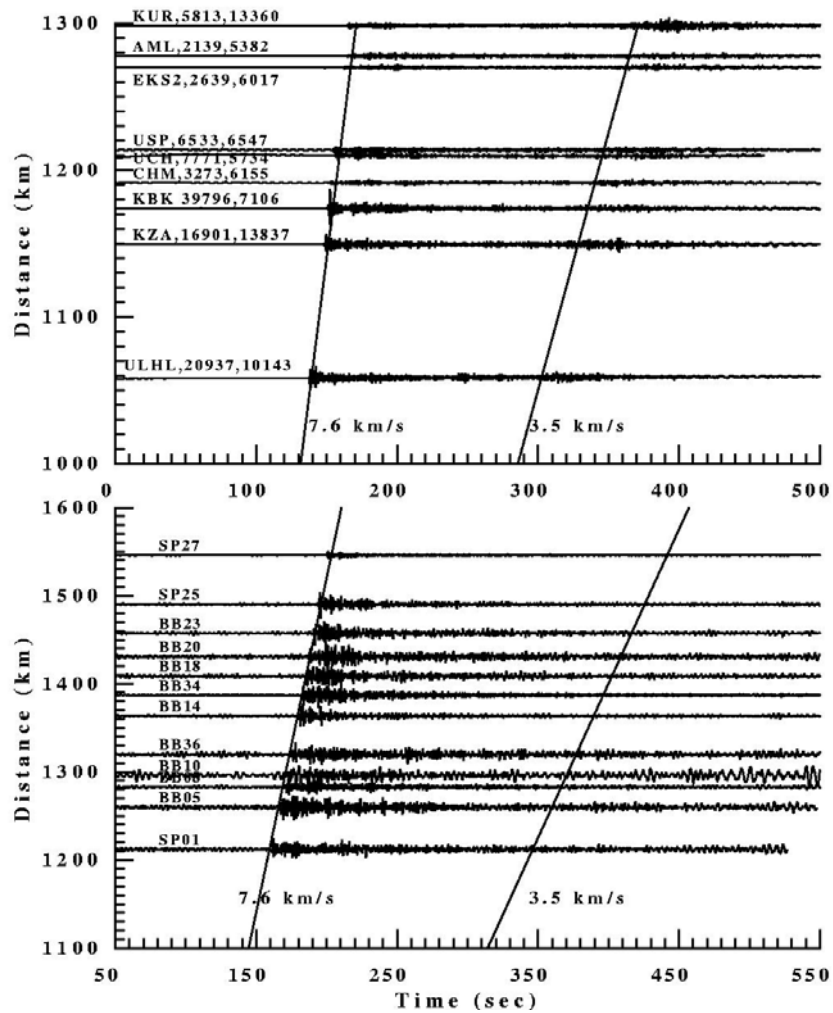


Figure 2. (Top) Record section from the October 7, 1994 explosion (mb=5.9) across the KNET. Station names, maximum Pn and Lg amplitudes in digital counts are written near the traces. The instrument gains are unified. The maximum Pn amplitude at KBK is about 19 times greater than that at AML. (Bottom) Record section from the same explosion but across the INDEPTH II array. Note the Lg is blocked.

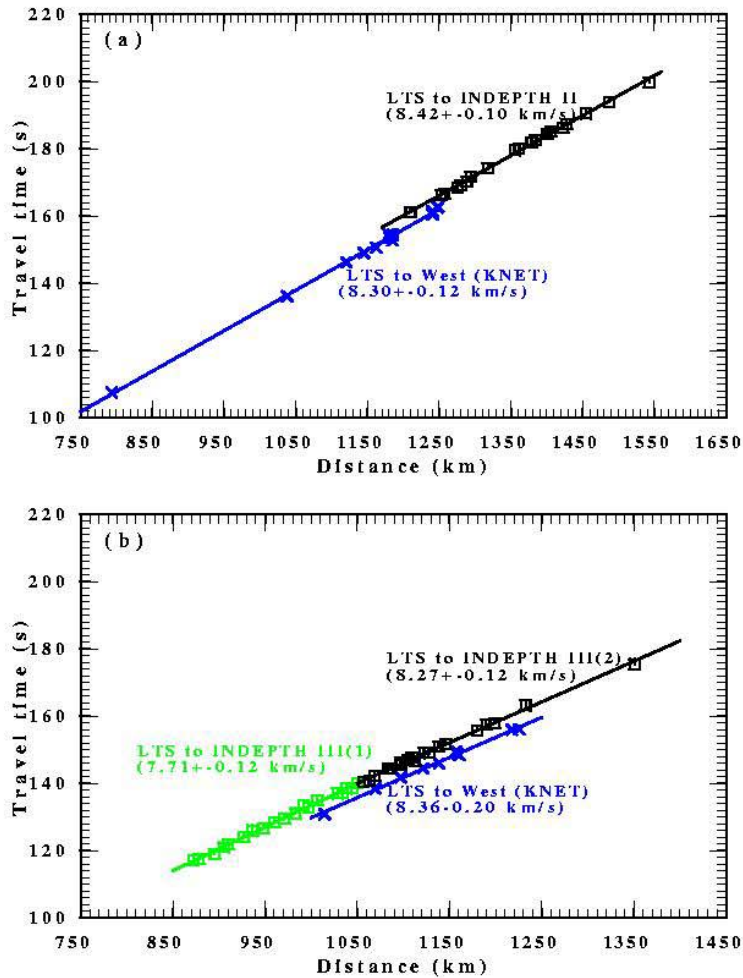


Figure 3. (a) Pn travel times from the October 7 Lop Nor Test Site (LTS) explosion to the INDEPTH II array (squares) and the KNET stations (crosses). Straight lines are linear regression fit for apparent Pn velocities. (b) Pn travel times from the January 30 LTS earthquake to the INDEPTH III sub-arrays (1) and (2) that are composed of stations north and south of the BNS (see Figure 1), plotted as squares (crosses). Straight lines are linear regression fit for apparent Pn velocities.

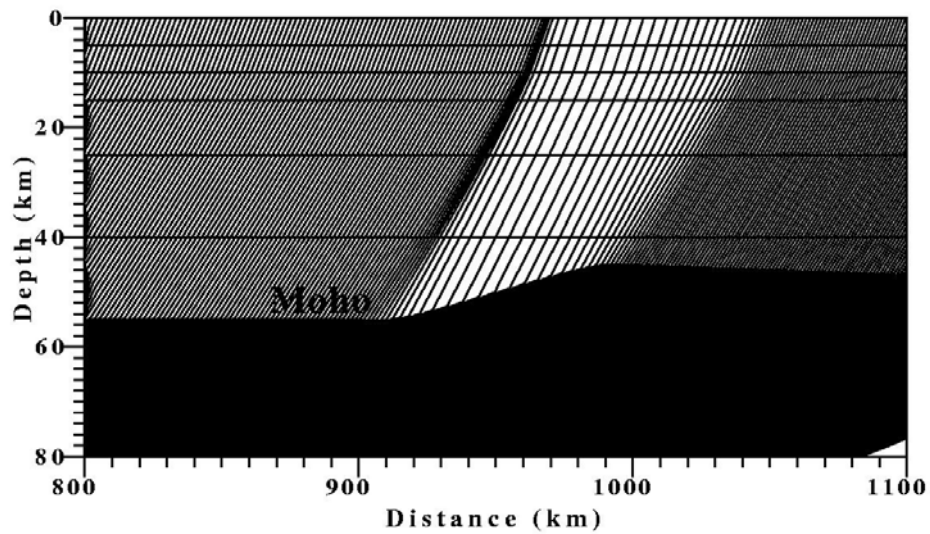


Figure 4. Pn ray pattern in a model for Tianshan by Rocker et al. (1993) that is modified from the Model M1 by adding a 2-D Moho topography. The ray tracing is conducted to simulate the focusing/defocusing effect by a Moho thinning under Lake Issyk-Kul and may be more complex (3-D) producing a more pronounced focusing/defocusing to Pn. We consider such Moho thinning the most likely cause of the large variability in Pn amplitude across the KNET.

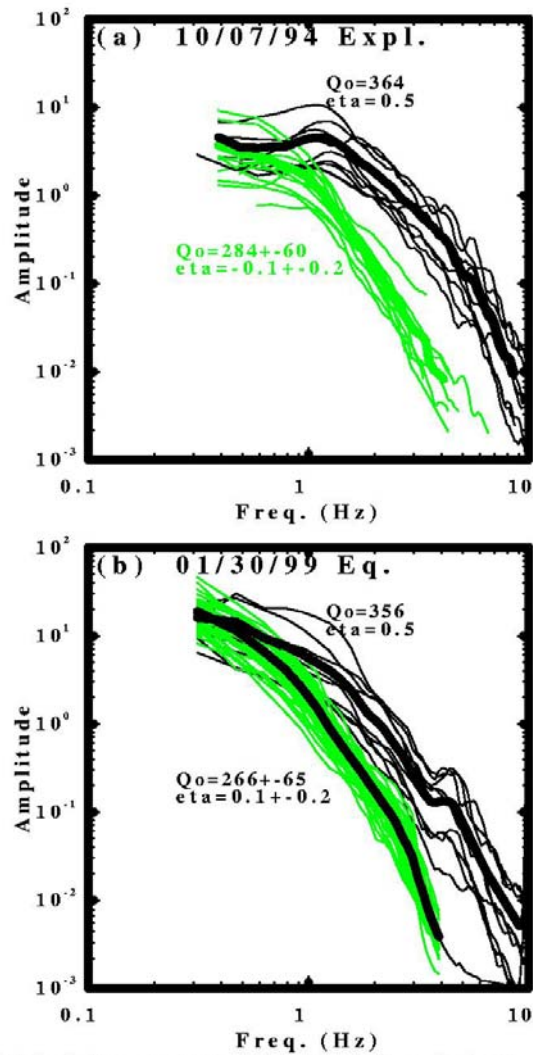


Figure 5. Individual Pn spectra (thin curves) and their array-average (thick curves). Panels (a) and (b) are spectra from the October 7, 1994 explosion and the January 30, 1999 earthquake, respectively. Black curves are for paths to the west (KNET array). Green curves are for the paths to the south (the INDEPTH II and III arrays in panels (a) and (b), respectively). Average Pn Q_0 and η to the west and south are written near the curves. Note the apparent spectral overshoot in the curves in (a).